NOVA SCHOOL OF SCIENCE & TECHNOLOGY

DEPARTMENT OF PHYSICS

X-RAY RESONANT RAMAN SCATTERING

SPECTRA SIMULATION FROM FIRST PRINCIPLES FOR COPPER BELLOW IONIZATION THRESHOLD USING HIGH-PERFORMANCE COMPUTING

GONÇALO GARCÊS SOBREIRA RODRIGUES BAPTISTA

BSc in Physics Engineering

DOCTORATE IN PHYSICS ENGINEERING

NOVA University Lisbon
September, 2023

NOVA SCHOOL OF
SCIENCE & TECHNOLOGY

DEPARTMENT OF
PHYSICS

X-RAY RESONANT RAMAN SCATTERING

SPECTRA SIMULATION FROM FIRST PRINCIPLES FOR COPPER BELLOW IONIZATION THRESHOLD USING HIGH-PERFORMANCE COMPUTING

GONÇALO GARCÊS SOBREIRA RODRIGUES BAPTISTA

BSc in Physics Engineering

Advisers: Jorge Felizardo Machado
Auxiliary Professor, NOVA University Lisbon
Mauro António Guerra
Auxiliary Professor, NOVA University Lisbon

Examination Committee

Chair: Name of the committee chairperson
Full Professor, FCT-NOVA

Rapporteur: Name of a rapporteur
Associate Professor, Another University

Members: Another member of the committee
Full Professor, Another University
Yet another member of the committee
Assistant Professor, Another University

DOCTORATE IN PHYSICS ENGINEERING

NOVA University Lisbon
September, 2023

X-ray resonant Raman scattering
Spectra simulation from first principles for Copper bellow ionization threshold using high-performance computing

This document was created with the (pdf/Xe/Lua)LaTeX processor and the NOVAthesis template (v7.0.3) [**novathesis-manual**].

Acknowledgements

Acknowledgments are personal text and should be a free expression of the author.

However, without any intention of conditioning the form or content of this text, I would like to add that it usually starts with academic thanks (instructors, etc.); then institutional thanks (Research Center, Department, Faculty, University, FCT / MEC scholarships, etc.) and, finally, the personal ones (friends, family, etc.).

But I insist that there are no fixed rules for this text, and it must, above all, express what the author feels.

”

“Sometimes I’ll start a sentence, and I don’t even know where it’s going.
I just hope I find it along the way.
Like an improv conversation.
An improversation.”

— Michael Scott, The Office
(Regional Manager of Dunder Mifflin Scranton)

”

“all work and no play makes Jack a dull boy
all work and no play makes Jack a dull boy
all work and no play makes Jack a dull boy
all work and no play makes Jack a dull boy
all work and no play makes Jack a dull boy
all work and no play makes Jack a dull boy
all work and no play makes Jack a dull boy
all work and no play makes Jack a dull boy
all work and no play makes Jack a dull boy
all work and no play makes Jack a dull boy
all work and no play makes Jack a dull boy
all work and no play makes Jack a dull boy
all work and no play makes Jack a dull boy
all work and no play makes Jack a dull boy
all work and no play makes Jack a dull boy
all work and no play makes Jack a dull boy
all work and no play makes Jack a dull boy
all work and no play makes Jack a dull boy
all work and no play makes Jack a dull boy
all work and no play makes Jack a dull boy
all work and no play makes Jack a dull boy
all work and no play makes Jack a dull boy
all work and no play makes Jack a dull boy
all work and no play makes Jack a dull boy
all work and no play makes Jack a dull boy
all work and no play makes Jack a dull boy
all work and no play makes Jack a dull boy
all work and no play makes Jack a dull boy
all work and no play makes Jack a dull boy
all work and no play makes Jack a dull boy
all work and no play makes Jack a dull boy
all work and no play makes Jack a dull boy
all work and no play makes Jack a dull boy
all work and no play makes Jack a dull boy
all work and no play makes Jack a dull boy
all work and no play makes Jack a dull boy
all work and no play makes Jack a dull boy
all work and no play makes Jack a dull boy
all work and no play makes Jack a dull boy
all work and no play makes Jack a dull boy
all work and no play makes Jack a dull boy
all work and no play makes Jack a dull boy
all work and no play makes Jack a dull boy
allworkandnoplaymakesJackadullboy
all work and no play makes Jack a dull boy
all work and no play makes Jack a dull boy
all work and no play makes Jack a dull boy
all work and no play makes Jack a dull boy
all work and no play makes Jack a dull boy
all work and no play makes Jack a dull boy
all work and no play makes Jack a dull boy
all work and no play makes Jack a dull boy
all work and no play makes Jack a dull boy
all work and no play makes Jack a dull boy
all work and no play makes Jack a dull boy
all work and no play makes Jack a dull boy
all work and no play makes Jack a dull boy
all work and no play makes Jack a dull boy
all work and no play makes Jack a dull boy
all work and no play makes Jack a dull boy
all work and no play makes Jack a dull boy
all work and no play makes Jack a dull boy
all work and no play makes Jack a dull boy
all work and no play makes Jack a dull boy
all work and no play makes Jack a dull boy
all work and no play makes Jack a dull boy
all work and no play makes Jack a dull boy
all work and no play makes Jack a dull boy
all work and no play makes Jack a dull boy
all work and no play makes Jack a dull boy
”

— **Jack Torrance**, The Shinning
(Caretaker of the Overlook)

Abstract

The work performed on this thesis comes as part of the effort to further understand the highly convoluted structure present on Copper's X-ray emission spectra, where, as with many other transition metals, a skewness can be observed on the $K_{\alpha_{1,2}}$, K_{β} and L transition lines. These lines originate due to the radiative relaxation of the atom's electronic structure post-ionization of inner shell electrons. However, it is very likely that the observed skewness is due to copper's satellite states' transitions.

Throughout this thesis, a study will be performed for the satellite states formed by the excitation of the inner-shell electrons, where, as opposed to the ionization process, usually considered in X-ray calculations, a photoexcitation process occurs.

Multiple atomic structure calculations will be performed using the *ab initio* state of the art Multiconfiguration Dirac-Fock General Matrix Elements (*MCDFGME*) code for different excited states configurations.

The obtained results will then be used in the analysis of experimental data obtained from a High-Precision Double Crystal Spectrometer (DCS), using a synchrotron X-ray source.

Due to the complexity of the calculations, the process can become substantial in terms of computational power and time. Therefore, further similar and more complex studies will be performed by implementing and running a script in the *Oblivion* supercomputer located at the University of Évora.

Keywords: Atomic Excitation, X-ray lines, *MCDFGME*, DCS, High Performance Computing

Resumo

asdasdasdasd

Contents

List of Figures

List of Tables

Listings

Glossary

Feynman Diagram 2D diagram depicting various physical interactions between elementary particles. Fermions are depectied as straight lines and bosons as wavy lines. *(p. 38)*

four-vector Vector used in special relativity composed of 4 components, one scalar time-like, and three vectorial space-like. These vectors behave in special way, such as their norm being Lorentz invariant. Can be written in covariant, X_μ, and contravariant form, X^μ, with the difference being the sign of the time-like components. Example of a contravariant four vector: $X^\mu = (X^0, X^1, X^2, X^3) = (X^0, \boldsymbol{X})$ *(pp. xiv, 9)*

Lorentz invariant A Lorentz invariant scalar, obtained, for example, from a Minkowski norm, does not change when operated by a Lorentz Transformation. *(pp. xiv, 9)*

Minkowski norm Yields the Lorentz Invariant norm for a four-vector: $p_\mu p^\mu$. Equivalent to the dot product of a classical vector. *(pp. xiv, 9)*

self consistency method The electron wavefunctions go through a variational process in order to reach convergence for an energetic minimum. *(p. 7)*

virtual photons While in reality, during a Coulomb interaction, 'real' particles are not exchanged, the electromagnetic field is still mediated by photons. This way virtual photons are tools used in order to better represent electromagnetic interactions. *(p. 11)*

Acronyms

Grasp2k	General-purpose Relativistic Atomic Structure Package 2k *(p. 13)*
MCDFGME	Multiconfiguration Dirac-Fock General Matrix Elements *(pp. vi, viii, ix, 12–15, 18)*
MCDF	Multiconfiguration Dirac-Fock *(pp. viii, 11, 18)*
MPI	Message Passing Interface *(pp. ix, 22)*
ASC	Atomic Structure Calculations *(pp. ix, 30)*
DCS	Double Crystal Spectrometer *(p. vi)*
EMF	Electromagnetic Field *(pp. 6, 11, 17)*
FAC	Flexible Atomic Code *(p. 13)*
HF	Hartree-Fock *(p. 8)*
HPC	High Performance Computing *(pp. ix, 30)*
QED	Quantum Electrodynamics *(pp. viii, 2, 11, 14, 18)*

Todo list

Chapter 1

Theoretical Introduction

Falta introdução? Meter a conversa dos FP de 2008

Throughout this thesis, different topics regarding Quantum Mechanics, Atomic Physics and spectroscopy will be approached, hence why a theoretical introduction is needed. In it, themes such as the characteristic X-rays of elements, the relativistic Dirac equation and QED corrections and methods for solving the many-body problem will be discussed.

1.1 Characteristic X-rays

When subjected to a high energy beam of particles (usually photons or electrons), an element may go through the process of the ionization of inner-core electrons, which is followed by the emission of radiation of its own, in the form of X-rays and/or Auger electrons. The radiation emitted throughout this process presents well-defined energy values and thus provides a way to ascertain if an element is present in a sample under study. Due to this reason, these characteristic emissions are of an extremely high importance in a wide range of scientific areas.

When an atomic system is in a bound state, the electrons orbiting the nucleus are occupying fixed quantum states, defined by their principal atomic number, n, angular momentum, l, and spin, s. Electrons are also fermions, and thus must respect Pauli's exclusion principle, each occupying a single state, only occupied by that single electron. These quantum numbers provide information about each electron's wavefunction, and the collection of all the electrons' wavefunctions can be used in order to describe the whole system. When operating the Hamiltonian on this collection of wavefunctions, the atomic system's state's energy is obtained. Besides all the occupied states, an infinite more number of possible eigenfunctions will compose that system's base.

1.1.1 Ionization as a vacancy generator

As previously mentioned, X-ray fluorescence spectroscopy has many uses and applications in a wide range of scientific areas. In this form of spectroscopy, the element at study, composed of a nucleus and N orbiting electrons, is bombarded with radiation leading to the ionization of inner-shell electrons while leaving a vacancy in their place (Figure 1.1).

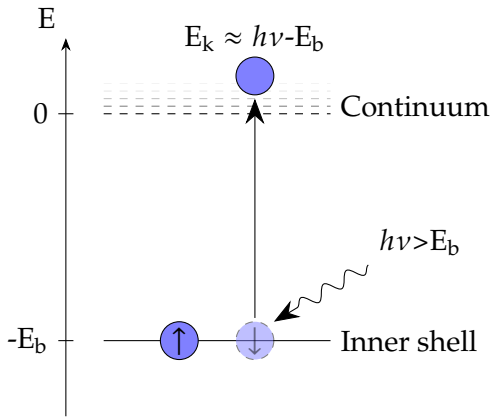

Figure 1.1: Photoionization.

The atomic structure, now composed of $N-1$ electrons, will be left in an energetically unstable state, due to there being other possible lower energy states. This will lead to various processes of atomic relaxation, where the system will rearrange itself in order to find a lower energy configuration.

The main processes for this rearrangement are two competing decay paths: radiative relaxation, and Auger electron emission.

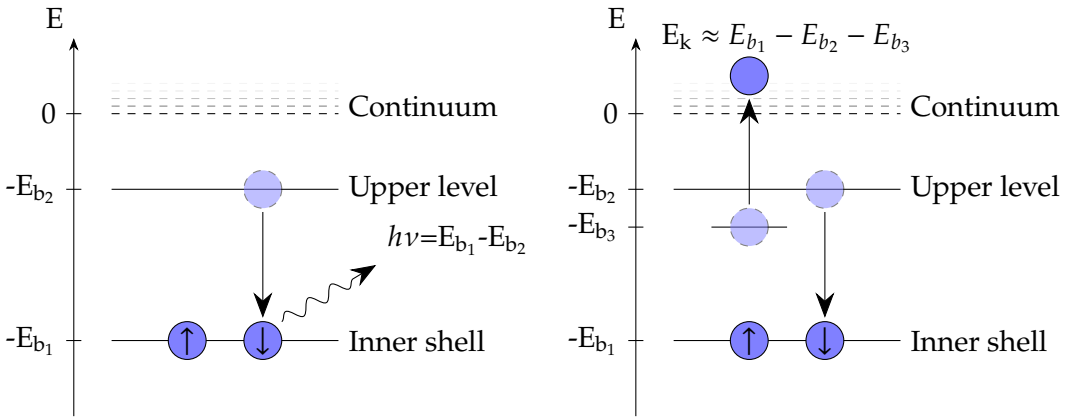

(a) Radiative Decay

(b) Auger Transition

Figure 1.2: Principal atomic relaxation processes.

In the case of radiative relaxation, an upper shell electron will move and occupy the hole left in the inner shell. During this process, energy is released through the emission of photons with energy in the range of X-rays. The detection of these photons is what allows for an analysis and detection of the element at study.

On the other hand, an Auger emission occurs when in the process of an upper electron shifting to a shell hole, energy is released not in the form of photons, but by the atomic system going through the process of the ionization of a lesser bound electron.

In reality, when the initial vacancy is generated, two more processes can occur: shake-off and shake-up. Due to a sudden change in the potential felt by the remaining electrons,

whilst going through the ionization, one other electron may become unbound, leading to a second ionization, the shake-off process, or may be excited to an upper state, during shake-up. These processes' occurrence probabilities are related to the rate at which the electron leaves the system during the first ionization. For lower electron emission energies, where the ionization process is rather "slow", and there is not much energy for shake up/off to occur, the adiabatic regime reigns. In this regime, the shake probabilities are small, and increase with the beam's energy. For higher energies, the transition occurs in the sudden regime, where the electrons' exit can be considered instantaneous. Now, while the shake probabilities still increase with the energy of the beam, they quickly saturate for a maximum value of probability, which can be calculated by computing overlaps between the electrons' initial and final states. These processes, however, are out of scope for this thesis, but should the reader be interested, the model conceived by Thomas [1] predicts the shake probability as a function of energy.

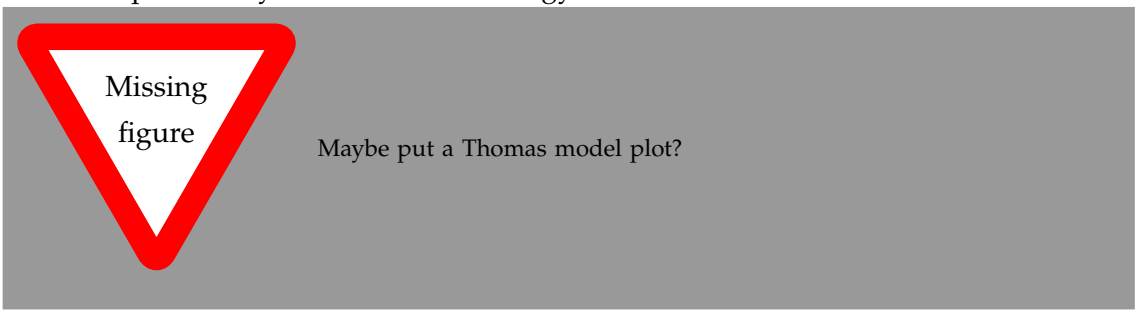

1.1.2 Transition notation

The characteristic radiation measured from the radiative relaxation of a post-ionization unstable atomic system is one of the main ways of identifying an atomic element. This is due to the photons emitted possessing quantized values of energy, forming well-defined energy lines when observed in a spectrometer. In order to understand the change that occurred in the atomic system which lead to a specific emission, the spectral lines get labels based on a notation which usually takes into account the initial and final orbitals where the vacancy was present. A very illustrative diagram, exemplifying some transitions can be found in Appendix B.

Throughout this thesis, Siegbahn notation will be used, for the most part, but should the reader prefer IUPAC's, Table 1.1 has the conversion between notations.

1.1.3 Excitation as a vacancy generator

As previously mentioned, throughout this thesis, while the study is focused on the characteristic radiation emitted during an atomic relaxation process, the main vacancy generation method at study shall be the photoexcitation process (Figure 1.3), instead of ionization. The levels obtained after a photoexcitation of core shell electrons has occurred could be some of the many so-called satellite states, where the electronic configuration present during the relaxation process contains additional electrons or holes, or is simply not

Table 1.1: Siegbahn VS IUPAC notation. Adapted from [2].

Siegbahn	IUPAC	Siegbahn	IUPAC	Siegbahn	IUPAC
K_{α_1}	$K-L_3$	L_{α_1}	L_3-M_5	L_{γ_1}	L_2-N_4
K_{α_2}	$K-L_2$	L_{α_2}	L_3-M_4	L_{γ_2}	L_1-N_1
K_{β_1}	$K-M_3$	L_{β_1}	L_2-M_4	L_{γ_3}	L_1-N_2
$K^I_{\beta_2}$	$K-N_3$	L_{β_2}	L_3-N_5	L_{γ_4}	L_1-O_3
$K^{II}_{\beta_2}$	$K-N_2$	L_{β_3}	L_1-M_3	$L_{\gamma'_4}$	L_1-O_2
K_{β_3}	$K-M_2$	L_{β_4}	L_1-M_2	L_{γ_5}	L_2-N_1
$K^I_{\beta_4}$	$K-N_5$	L_{β_5}	$L_3-O_{4,5}$	L_{γ_5}	L_2-O_4
$K^{II}_{\beta_4}$	$K-N_4$	L_{β_6}	L_3-N_1	L_{γ_8}	L_2-O_1
$K^x_{\beta_4}$	$K-N_4$	L_{β_7}	L_3-O_1	$L_{\gamma'_8}$	$L_2-N_{5,6}$
$K^I_{\beta_5}$	$K-M_5$	L_{β_8}	$L_3-N_{6,7}$	L_η	L_2-M_1
$K^{II}_{\beta_4}$	$K-M_4$	L_{β_9}	L_1-M_5	L_l	L_3-M_1
		L_{β_9}	L_1-M_4	L_s	L_3-M_3
		L_{β_9}	L_3-N_4	L_t	L_3-M_2
		L_{β_9}	L_2-M_3	L_u	$L_3-N_{6,7}$
				L_v	$L_2-N_{6,7}$

the standard configuration when talking about characteristic emissions. The characteristic radiation from transitions that originated from these states are one of the keys needed to fully comprehend and deconvolute an element's emission spectra.

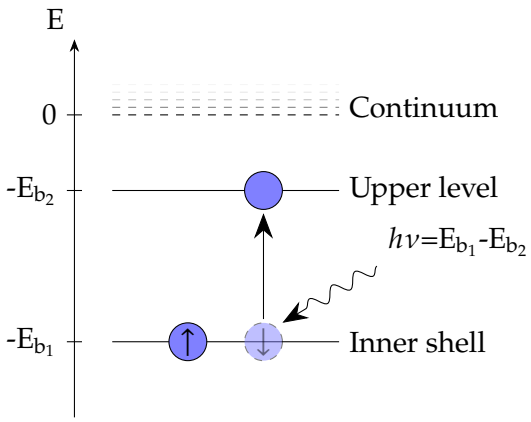

Figure 1.3: Resonant Photoexcitation

1.2 Radiative transitions

In terms of quantum mechanics, the properties of a system's change of state can be derived using perturbation theory, where a change in energy can be treated as perturbation, and takes into account the conservation laws physical properties, such as the angular momentum of the system as basis for the selection rules.

The transition's radiation type can be of two main flavors, Electric, E_k, or Magnetic, M_k,

with k representing its multiplicity. These labels indicate which of the Electromagnetic Field (EMF) component had the strongest influence on the transition's occurrence. For both these types of transitions, the system's total angular momentum is allowed a change of $\Delta J = 0, \pm k$, and so does its projection, M_J. However, different transitions lead to different changes of parity in the system and to different selection rules.

It should also be of note that, usually, for the same multiplicity, an E transition is more intense than an M, and that it is also possible for rare 2-photon transitions to take place, where a combination of different transition types can occur.

The intensity of a transition is proportional to the squared norm of the perturbation's matrix element involving the initial and final state $\left(\Gamma_{if} \propto \left|\langle\psi_i|H'|\psi_f\rangle\right|^2\right)$. It should also be noted that the electron's initial state population will serve as a scaling factor for the transitions' rate. For example, while the transition rate for a $2p_{1/2} \rightarrow 1s$ and $2p_{3/2} \rightarrow 1s$ should be about the same, the orbital $2p_{3/2}$ has double the population $2p_{1/2}$ has, hence why the K_{α_2} line has about half the K_{α_1} line's intensity.

One should also mention that monochromatic transitions do not exist. While the transition might have a well-defined energy, calculated by the difference in energy between the initial and final levels, due to Heisenberg's uncertainty principle, $\Delta E \Delta t > \frac{\hbar}{2}$, there will exist a natural energy broadening, the transition's natural width. The shapes representing these transitions are given by a Lorentzian distribution.

1.3 Solving the atomic many-body problem

When studying a system composed of multiple charged bodies, one must consider all the existing interactions. Whilst there are known analytical solutions for 2-bodies Hydrogenoid systems, with the presence of more non spatially-bound particles, the Coulomb interaction pairs lead to the impossibility of finding a set of analytical wavefunctions which are a part of the Hamiltonian's eigenset. Consecutively, the need for a numerical method that is able to compute solutions for these complex systems arose.

1.3.1 The non-relativistic Hamiltonian

The first approach used in order to solve the many-bodies problem used a non-relativistic consideration. This way, the Hamiltonian consists on the sum of the system's non-relativistic momentum-related energies and the energy of Coulomb interactions between all the bodies in the system, while considering the nucleus as fixed in space, due to it being thousands of times more massive than the orbiting electrons.

Essentially, and in atomic units:

$$\underbrace{\sum_{i}^{N} \overbrace{\frac{1}{2}\nabla_i^2}^{E_1} \overbrace{-\frac{Z}{r_i}}^{E_2}}_{\text{Individual Hamiltonian}} + \underbrace{\sum_{i<j}^{j} \overbrace{\frac{1}{r_{ij}}}^{E_3}}_{\text{Pair repulsion}},$$

$E_1 \rightarrow$ Momentum $\quad E_2 \rightarrow e^- $nuc. Coulomb attraction $\quad E_3 \rightarrow e^- e^-$ Coulomb repulsion (1.1)

1.3.2 The Hartree-Fock Method

This numerical method is one of the staple and most enduring procedures for solving the problem associated with a many-body system. As a side note, an in-depth explanation on all the intricacies of this method can be found in many of the literature, but as for the writing of this thesis, the works [3–6] were the ones consulted.

Hartree developed an iterative method, further enhanced by Fock and Slater, based on the field's self consistency method. In this approach, when studying a multi-electronic system, such as an atom, each electron's wavefuction is composed as a product of a spacial part, ψ, and one related to the electron's spin, χ, as to be able to account for Pauli's exclusion principle and, if so desired, relativistic effects.

$$u = \psi\chi, \tag{1.2}$$

The wavefuction capable of describing the whole system, Ψ, should be somewhat of a product of all the wavefunctions describing each individual electron. However, one must not forget the need for this wavefunction to respect the antisymmetry principle, due to the electron's fermionic nature. In order to achieve this, Ψ is to be composed of a Slater determinant:

Explain anti-symmetry and put it in the glossary

Explain in the glossary

$$\Psi = \frac{1}{\sqrt{N!}} \begin{vmatrix} u_1(x_1) & u_2(x_1) & \cdots & u_N(x_1) \\ u_1(x_2) & u_2(x_2) & \cdots & u_N(x_2) \\ \vdots & \vdots & \ddots & \vdots \\ u_1(x_N) & u_2(x_N) & \cdots & u_N(x_N) \end{vmatrix}, \tag{1.3}$$

It is of high importance that the set of basis wavefunctions respects orthonormality. These are to be initialized as trial wavefunctions for the numerical method.

The main goal for this algorithm is to, as per the self consistency method, follow the variational principle with the goal of minimize a functional, as a way of reaching an energetic minimum. This optimal, yet unknown energy, E_0 (calculated by operating the Hamiltonian on the system's optimal wavefunctions), will attempt to be reached by the variation of the trial wavefunctions that provide a non-minimized solution. Whilst the optimal wavefunctions will never be reached, the purpose of this method is to reach a

solution that yields an energetic value as close as possible to E_0, while always yielding $\langle\Psi|H|\Psi\rangle \geq E_0$, due to the numerical nature of the method.

The computational method consists on starting with the previously mentioned trial wavefunctions and employing them in the Hartree-Fock's potential calculation through the Hartree-Fock (HF) equations.

Finish the explanation

In an over-simplistic scheme, the self-consistent Hartree-Fock computational method can be represented by the block diagram in Figure 1.4.

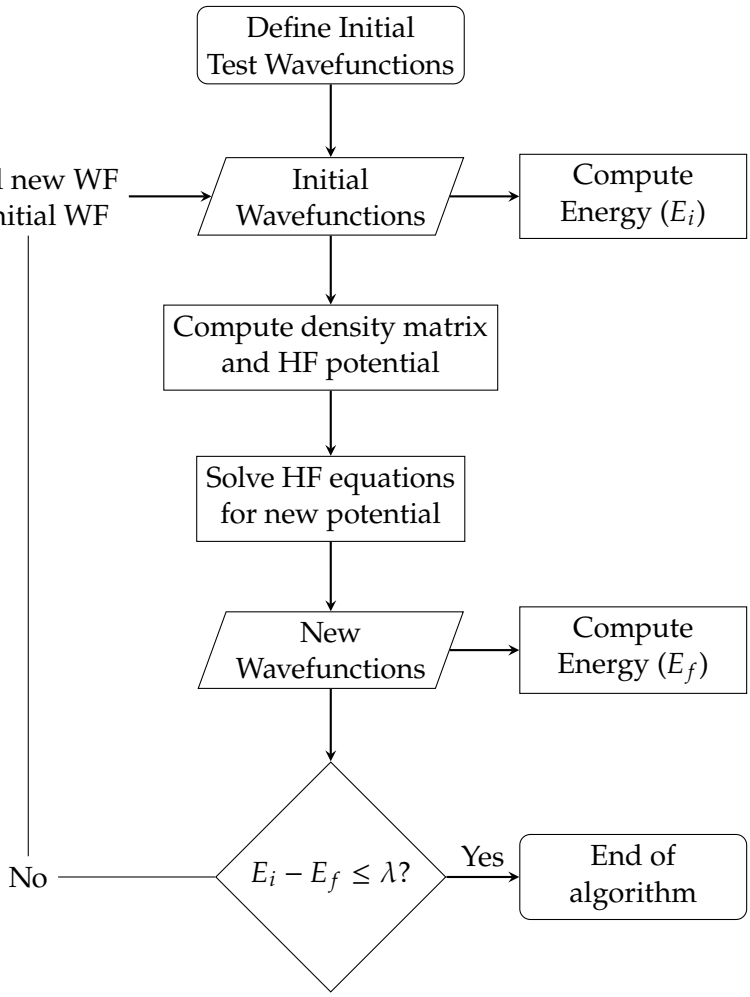

Figure 1.4: HF method's block diagram.

1.3.3 The Dirac Equation

While Schrödinger's equation may be one of the most significant and impactful equations in Modern Physics, it is also not free of its of limitations. The fact that it does not account for the existence of the electron's spin and the lack of consideration of relativistic effects are some of the most impactful setbacks. Consulting the works in [7–10], this work will follow an exploration of different approaches that followed in order to solve the aforementioned problem.

Many scientists, such as Klein, Gordon and later Fock, had already conceived a relativistic correction to Schrödinger's equation, where the free-particle energy makes use of the relativistic momentum-energy relation, as displayed in equation (1.4).

$$E = \sqrt{c^2\boldsymbol{p}^2 + m^2c^4}, \tag{1.4}$$

This notable definition can be derived from the Lorentz invariant scalar produced by Minkowski norm of the momentum four-vector (1.5).

$$p^\mu p_\mu = m^2c^2 \Leftrightarrow \frac{E^2}{c^2} - \boldsymbol{p}^2 = m^2c^2 \Leftrightarrow \frac{E^2}{c^2} = \boldsymbol{p}^2 + m^2c^2, \tag{1.5}$$

Now, inputting this new energy operator into Schrödinger's equation, yields the Klein-Gordon equation (1.6), allowing for Schrödinger's equation to now be Lorentz-invariant (proof can be found in Strickland's book [11]).

$$-\hbar^2\frac{\partial^2}{\partial t^2}\boldsymbol{\psi} = \left(-c^2\hbar^2\nabla^2 + m^2c^4\right)\boldsymbol{\psi}, \tag{1.6}$$

This new approach was, however, still limited, as it only described spin 0 particles (e.g., some mesons), and made use of a second order derivative in the time-like component.

Try to explain why this might be a problem

Came 1928 and a new equation was developed by Paul Dirac [12], one taking now into account not the classical 3 dimensional space components, but the relativistic four components.

Dirac started by rewriting the energy-momentum relation, ending up with an equivalent equation (1.7), employing 4×4 matrices, due to the 4 relativistic dimensions at play, and incorporating spins into the equation by making use of the Pauli matrices (1.9).

$$E = c\boldsymbol{\alpha}\cdot\boldsymbol{p} + \beta mc^2, \quad \boldsymbol{\alpha} = (\alpha_1, \alpha_2, \alpha_3), \tag{1.7}$$

$$\alpha_i = \begin{pmatrix} 0 & \sigma_i \\ \sigma_i & 0 \end{pmatrix} \qquad \beta = \begin{pmatrix} I_2 & 0 \\ 0 & -I_2 \end{pmatrix} \qquad I_2 = \begin{pmatrix} 1 & 0 \\ 0 & 1 \end{pmatrix}, \tag{1.8}$$

$$\sigma_1 = \begin{pmatrix} 0 & 1 \\ 1 & 0 \end{pmatrix} \qquad \sigma_2 = \begin{pmatrix} 0 & -i \\ i & 0 \end{pmatrix} \qquad \sigma_3 = \begin{pmatrix} 1 & 0 \\ 0 & -1 \end{pmatrix}, \tag{1.9}$$

In order to fully comprehend this shift of notation, one should equate the square of the two equations, (1.4) and (1.7), and confirm its validity.

$$c^2\boldsymbol{p}^2 + m^2c^4 = c^2\boldsymbol{\alpha}^2\boldsymbol{p}^2 + 2mc^3\boldsymbol{\alpha}\cdot\boldsymbol{p}\cdot\beta + \beta^2m^2c^4, \tag{1.10}$$

In order for this equation to make sense, the following conditions must be true ~~(which in fact, they are)~~:

do the demonstration, dummy

$$\begin{cases} c^2\boldsymbol{p}^2 = c^2\boldsymbol{\alpha}^2 p^2 & \Leftrightarrow \boldsymbol{\alpha}^2 = 1 \\ 0 = 2mc^3 p\boldsymbol{\alpha}\beta & \Leftrightarrow \boldsymbol{\alpha}\beta = 0\,, \\ m^2c^4 = \beta^2 m^2 c^4 & \Leftrightarrow \beta^2 = 1 \end{cases} \tag{1.11}$$

Taking the previous considerations into account, one can now construct Dirac's free-particle equation (1.12):

$$i\hbar\frac{\partial}{\partial t}\boldsymbol{\psi} = \left(c\,\boldsymbol{\alpha}\cdot\boldsymbol{p} + \beta mc^2\right)\boldsymbol{\psi} = \begin{pmatrix} mc^2 I_2 & -i\hbar c\,\boldsymbol{\sigma}\cdot\boldsymbol{\nabla} \\ -i\hbar c\,\boldsymbol{\sigma}\cdot\boldsymbol{\nabla} & -mc^2 I_2 \end{pmatrix}\cdot\begin{pmatrix} \psi_1 \\ \vdots \\ \psi_4 \end{pmatrix}, \tag{1.12}$$

This equation, however, as mentioned above, can only describe a single particle present in a field-free region. In order to account for the existence of a field, such as the electromagnetic field, derived from the four-potential A^μ, composed by the electric scalar potential field, $A^0 = \phi$, and the vector potential, $(A^1, A^2, A^3) = \boldsymbol{A}$, the following change on the momentum four-vector must be made:

$$p^\mu \rightarrow p^\mu - eA^\mu, \quad A^\mu = \left(\phi, \boldsymbol{A}\right), \tag{1.13}$$

The Hamiltonian can now be rewritten as to account for the presence of the electromagnetic field (1.14). This way it is possible to include, for example, the electron-nucleus Coulomb attraction.

$$H_D = -e\phi + \beta mc^2 + \boldsymbol{\alpha}(c\boldsymbol{p} + e\boldsymbol{A}), \tag{1.14}$$

For a central fixed potential, as is the one generated by the nuclear charge, the 3 space-like components from the four-potential are null, and the time-like component, $\phi = \dfrac{Ze}{r}$. The Hamiltonian gains now a more recognizable form:

$$H_D = -\frac{e^2 Z}{r} + \beta mc^2 + \boldsymbol{\alpha}\cdot\boldsymbol{p}c, \tag{1.15}$$

A very interesting fact about Dirac's equation is that it yields, in fact, two sets of solutions: the large component (positive energy values), for particles, and the small component (negative energy values), for antiparticles.

1.3.3.1 The Dirac-Breit Equation

Once again, when considering a system composed of many bodies, one must consider all the present interactions, namely, the electron-electron repulsion in an atom. Breit, in 1929, had created a relativistic approach to treat the electron-electron interactions, consisting on a set of equations building upon the classical non-relativistic Hamiltonian from equation (1.1), which can be consulted in Appendix A. Breit's equations are able to

account for angular momenta couplings and estimate level energy splittings, the change of a particle's apparent mass as a function of velocity, and even include the interaction of an applied external magnetic field [10].

It is quite obvious Breit's equations introduce a great complexity in the search of the new Hamiltonian's eigenfunctions. Nonetheless, when trying to include an approximation of Breit's considerations into Dirac's equation, one must add the following operator to the one present in equation (1.15):

$$H_B = \sum_{i>j} \frac{e^2}{r_{ij}} - e^2 \left(\frac{\boldsymbol{\alpha}_i \boldsymbol{\alpha}_j}{r_{ij}} + \frac{(\boldsymbol{\alpha}_i \boldsymbol{\nabla}_i)(\boldsymbol{\alpha}_j \boldsymbol{\nabla}_j) r_{ij}}{2} \right), \tag{1.16}$$

This set of terms will account for the fact that Coulomb interactions, mediated by the electric field, and therefore, virtual photons, cannot occur at instantaneous velocities, but at the speed of light.

1.4 QED considerations

Falar aqui sobre as contribuições. Não tem que ser extensivo

Lorem ipsum dolor sit amet, consectetur adipiscing elit. Etiam ut justo justo. Cras pulvinar massa sollicitudin ligula faucibus, in vulputate magna viverra. Nulla risus ante, maximus ut nunc sit amet, condimentum convallis mi. Phasellus et mi aliquet, ornare sapien egestas, vehicula orci. Donec ac massa tempus, iaculis tortor vitae, tempus tortor. Donec nec justo eros. Sed mauris purus, facilisis eu tempus quis, mattis et erat. Sed et congue metus, in venenatis nibh. Nullam ipsum ex, scelerisque non nunc sit amet, ultrices commodo felis. Proin sodales turpis nulla, quis tincidunt leo auctor id. Ut ac nulla quis felis molestie ullamcorper. Nulla tristique dui velit, sit amet rutrum libero dignissim id.

In hac habitasse platea dictumst. Vivamus laoreet neque odio, vitae faucibus massa eleifend sit amet. Curabitur tempor facilisis velit, eget blandit nisi rutrum at. Morbi a massa a lacus lobortis ultricies eget vel enim. Ut augue nisl, tristique eget luctus eget, scelerisque vitae risus. Aliquam in felis et metus euismod porttitor. Nullam nec ligula mi. Aliquam non vulputate sem. Proin ut leo eget ex bibendum venenatis ac vel sapien. Cras felis eros, cursus quis dolor posuere, scelerisque tempus orci. In nec quam in dui efficitur aliquam vitae sit amet dui. Cras laoreet tellus vel risus molestie mattis. Nulla facilisi. Duis rutrum mauris vitae malesuada consequat.

Should the atomic system be subjected to an external EMF, the level structure would change due to Zeeman's and Stark's effects, allowing for the probing of the atom's hyperfine structure.

1.4.1 The *MCDF* Method

Ler bem o manual e explicar bem o método e todas as coisas diferentes que se podem fazer

As previously mentioned in section 1.3.2, there is a need for a numerical method in order to compute and find the eigenfunctions for a many-body Hamiltonian. While the Hartree-Fock method was able to reasonably solve the non-relativistic problem, now,

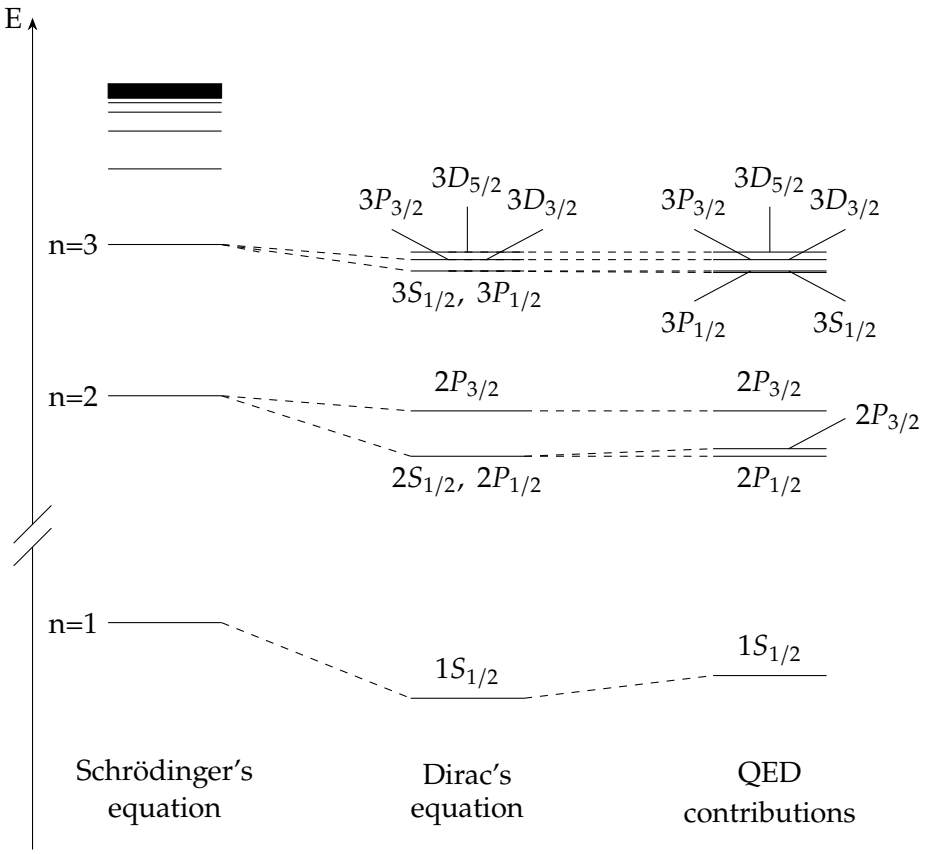

Figure 1.5: Comparison of Hydrogen level diagrams. Adapted from [13]

while considering the Dirac-Breit Hamiltonian from equations (1.15) and (1.16), there is a need for a new method.

Hence, the state of the art *MCDFGME* arises. This self-consistent iterative method, based on the same method present in section 1.3.2, is able to solve and find eigenfunctions for a multielectronic system, now taking into account the Dirac-Breit Hamiltonian. Moreover, it is also capable of incorporating electron correlation and many QED effects not yet considered in the relativistic equation, such as the Lamb-shift, vacuum polarization, and the electron's self energy. A brief description of these contributions can be found in appendix C

1.5 State of the Art

This really needs a re-do

1.5.1 Copper's characteristic X-rays

Copper is a dominant element in today's society. While most of its uses are day-to-day related, it also has a high prevalence in many physical areas, namely, copper's K_α transitions [14]. While these radiative transitions have been measured countless times, with very well recorded energy values [15–19]. It is also common knowledge Copper's K_α

lines do not have a symmetric distribution, since both K_{α_1} and K_{α_2} line display a negative (left-tailed) skewness. Due to this fact, most of the fitting models used in order to analyze both Copper's K_{α_1} and K_{α_2} transitions involve the usage of a Lorentzian doublet, for each line [20, 21]. While many associate these asymmetries due to satellite states formed by shake processes [14, 22], with some theoretical studies having been performed [23], some authors note it could be due to X-ray resonant Raman scattering [22]. This effect occurs when a sample is exposed to energies under to near the ionization threshold, when a bound electron is excited to an upper state [24]. While there are some studies exploring this topic, most are focused on the cascade of low energy transitions that follow the post-scattering excitation [25]. Nonetheless, a previous experimental study has been able to show that for Copper exposed to synchrotron radiation tuned to energies near K-shell's ionization energy, some K_{α_1} transitions demonstrated to be narrower than expected [26].

1.5.2 MCDFGME capabilities

It has been noted multiple times that *MCDFGME* code excels in atomic structure calculations of super-heavy elements and highly-charged ions, where relativistic and QED effects are in prevalence [27–29]. However, it has also been proven to be an excellent tool for the calculation of less ionized and lighter atomic systems [30].

In addition, the *MCDFGME* code is able to calculate radiative and auger transition rates for the calculated configurations, which can be used in the simulation of theoretical spectra, due to being able to compute the transition's intensity and natural width. Since it is able to perform calculations, even for exotic atoms, it can be used to further understand many QED phenomena, further exploring the limits of our theory, and it's comparison to experimental data [31].

It should also be of note that there are many other code alternatives. While *MCDFGME*, which is a close-source project, provides a very high precision in the performed calculations at a high computational cost, Flexible Atomic Code (FAC), is an open source code which requires less computational time for the calculations, however, it lacks *MCDFGME*'s precision, since it only is able to consider all the spin-orb couplings, but does not mix the possible configurations originating them. It can, however, calculate other collisional processes, such as electronic impact excitation cross-sections [32]. General-purpose Relativistic Atomic Structure Package 2k (*Grasp2k*) [33], and *AUTOSTRUCTURE* [34] are other codes with some of the same capabilities.

Chapter 2

Atomic Structure Calculations

In this chapter, the procedure that follows a standard atomic structure calculation will be discussed and explained in detail. Topics ranging from the usage of the *MCDFGME* code to compute quantities such as energy levels, orbital wavefunctions and transition rates, to the manner in which these parameters can be used in order to simulate a theoretical spectrum will be explored. All the information present in this chapter was obtained after a thorough study of *MCDFGME*'s manual [35].

2.1 The *MCDFGME* code's capabilities

As previously stated, *MCDFGME* is a program that allows for not only solving the many-body problem for an atomic system while making the proper QED energy corrections, but also for the computation of a great deal of atomic parameters. Consulting [36], one can see that these include, but are not limited to:

- Energy level calculations.
- Multipole radiative transition probabilities.
- Auger transition probabilities.
- Photoionization cross-sections.
- Electronic impact excitation cross-sections.
- Orbital wavefunction overlaps between same and different atomic systems.

meter mais cenas

2.2 The atomic system at study

Before proceeding to the explanation behind every step of the calculations performed, a previous discussion on the reason behind them should be had.

The main purpose of this thesis is that of simulating a theoretical spectrum for Copper's x-ray emission lines when subjected to a near ionization threshold x-ray source.

At this energy range, two main processes will be responsible for an electron moving out of a core-shell: Resonant photoexcitation, and ionization.

While the simulation of the theoretical spectra for ionized Copper would be quite straightforward (due to the low shake probabilities at near ionization threshold energies, transitions for satellite states were not incorporated in the simulation), the more extensive calculation is that of resonant photoexcitation.

Aside from ionized Copper, multiple atomic structure calculations were performed for many of Copper's first excited state configurations in order to consistently account for all possible decays from excited states.

In total, and in addition to ionized Copper, 18 different standalone calculations were performed for the case in which the atomic system has undergone the process of an excitation of any one of the constituent electrons to one of the following orbitals:

- 4s, 4p, 4d, 4f
- 5s, 5p, 5d, 5f, 5g
- 6s, 6p, 6d, 6f, 6g, 6h
- 7p, 8p, 9p

2.2.1 Selecting all possible orbital configurations

As to perform an atomic structure calculation, by making use of the *MCDFGME* code, the system's electronic configuration is needed, hence why, for each calculation, all the possible one-hole and two-holes [1] configurations need to be provided, along with their respective labels which are used as identifiers of the orbital where the hole is present during the calculations. For example, in the case of ground state Copper that went through the process of the excitation of one of its electrons to the orbital 4p, there are many possibilities for the original orbital from where the electron came from. For this case, an example of all possible 1-hole and 2-holes configurations can be found in Annex I. These are obtained by running a single hole, or two holes by all the orbitals present in the ground state configuration.

2.3 Level Calculations

Now that all configurations have been selected, the calculations can proceed.

The first and most influential, step needed in order to simulate theoretical spectra is the calculation of the level structure for all given configurations.

[1] These need to be considered due to describing the final state of the system after an Auger transition or Shake-off process. The Auger transition rates will be needed in order to compute the full width of the initial 1-hole level and diagram transitions.

This, however, is no simple task. Besides the given configuration, an atomic level is described by two other quantum numbers.

2.3.1 The level manifold

Prior to proceeding with the discussion, it is important to establish some of the notation that will be used throughout this thesis. In this work, where hyperfine splitting is not accounted for, an atomic level will be described by three sets of quantum numbers. These will be the parameters that will influence the system's energy levels.

Hole orbital labels $(n\ l_j)$ - This quantum number set is related to the system's electronic configuration and can be composed of one or more labels, indicators of the orbitals where electrons are missing. These labels may have no physical meaning on their own and are used in conjunction with files such as the one in Annex I in order to retrieve the system's electronic configuration. For demonstrative purposes, assuming an initial Copper's ground state configuration as a starting point, before any hole-generating processes, to be $1s^2\ 2s^2\ 2p^6\ 3s^2\ 3p^6\ 3d^{10}\ 4s^1$, the quantum number set in question can be used to describe various possible ionization configurations:

- $1s^1\ 2s^2\ 2p^6\ 3s^2\ 3p^6\ 3d^{10}\ 4s^1 \rightarrow (1s)$
- $1s^1\ 2s^1\ 2p^6\ 3s^2\ 3p^6\ 3d^{10}\ 4s^1 \rightarrow (1s, 2s)$

Total angular momentum number J - This number is the indicator of the total angular momentum of the atomic system, resulting from the couplings between the electrons' orbital angular momenta and spin. A single configuration can result in many coupling possibilities and, in turn, different values for J.

As an example, let's take that of Copper that underwent the excitation process of an electron from the 2p orbital to 4p, with an electron configuration of $1s^2\ 2s^2\ 2p^5\ 3s^2\ 3p^6\ 3d^{10}\ 4s^1\ 4p^1$. One can now easily observe there are three open orbitals, each with an uncoupled electron. The different coupling possibilities between these three electrons will generate four different possible total angular momentum values: $J = {}^1/_2,\ {}^3/_2,\ {}^5/_2,\ {}^7/_2$. In table 2.1, a coupling example will be given for each of them.

Table 2.1: Total angular momentum generated by different couplings

2p		4s		4p		Total/J
m_l	m_s	m_l	m_s	m_l	m_s	$m_l + m_s$
1	$-1/2$	0	$-1/2$	1	$-1/2$	$1/2$
1	$1/2$	0	$-1/2$	1	$-1/2$	$3/2$
1	$1/2$	0	$1/2$	1	$-1/2$	$5/2$
1	$1/2$	0	$1/2$	1	$1/2$	$7/2$

Lagrange multiplier ϵ - Indicator of the eigenvalue for the state on which the calculation will be performed on. The need for this quantum number arises from the fact that, even for the same configuration and the same total angular momentum, there are many possible arrangements that yield these quantum numbers. As an example, for the same configuration used previously, and assuming a total angular momentum $J = 5/2$, there are three different possible couplings that generate that value of angular momentum, as can be seen in table 2.2.

Table 2.2: Same total angular momentum generated by different configurations

$J = 5/2$					
2p		4s		4p	
m_l	m_s	m_l	m_s	m_l	m_s
1	$-1/2$	0	$1/2$	1	$1/2$
1	$1/2$	0	$-1/2$	1	$1/2$
1	$1/2$	0	$1/2$	1	$-1/2$

This splitting of quantum numbers for a given configuration gives origin to the level manifold (Figure 2.1), reason why, even for a simple calculation, hundreds to thousands of levels need to be calculated. It is also of note that, for a given Total angular momentum value, J, there are $2J+1$ states associated to it due to the angular momentum projection. In the presence of an external EMF, the hyperfine level structure would be observed, due to Zeeman and Stark's effects. However, for the purpose of this thesis, no external field was considered, and calculations were only done for the maximum total angular momentum projection value, with a $2J+1$ degeneracy taken into account in the following calculations.

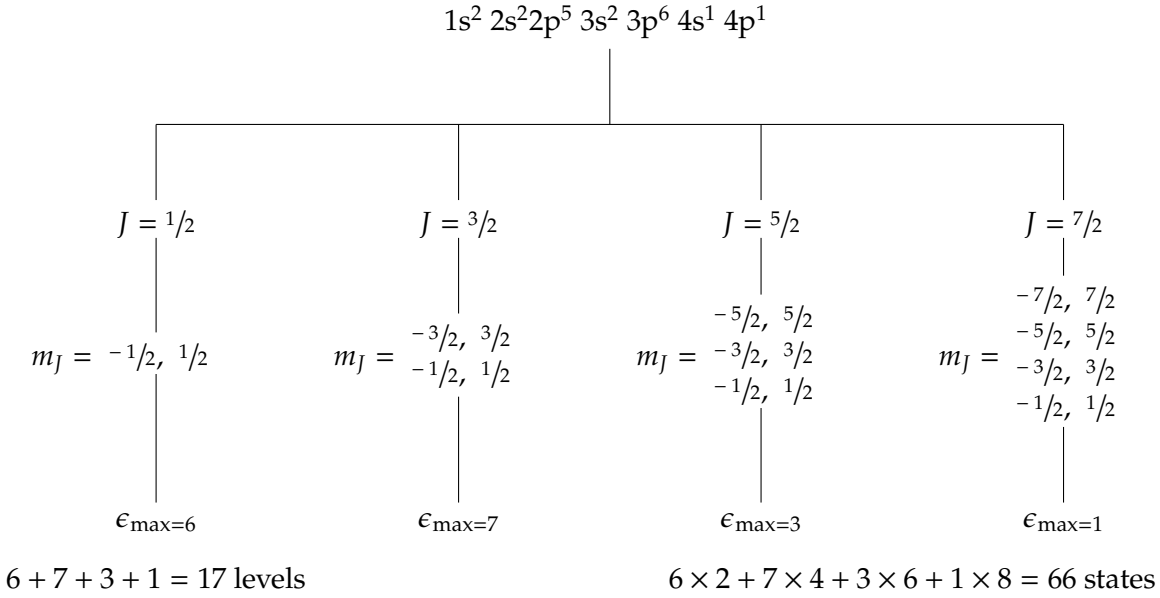

Figure 2.1: Splitting of quantum numbers for a given configuration.

In conclusion, an atomic level can be defined by the set of these three quantum numbers.

In the notation used throughout this thesis, a level will be identified by:

$$i \equiv \left[(n\ l_j)_i;\ J_i;\ \epsilon_i\right], \tag{2.1}$$

And the energy of the level:

$$E_i \equiv E\left[(n\ l_j)_i;\ J_i;\ \epsilon_i\right], \tag{2.2}$$

2.3.2 Level calculation with *MCDFGME*

Mention that the program works by the means of an input f05 file

Breit can be used as self consistent or perturbative

Talk about Lorentz and Coulomb gauges

A typical level calculation begins with the formatting of the input `.f05` file. This file contains the necessary information and instructions the program needs for the computation that follows when the executable `mcdfgme2019.exe` is called.

The input file has a certain input structure in which certain calculation parameters are defined. A previously tailored template input file is used, where, by default, the full Breit interaction is considered, with the magnetic and retardation parts, as well as vacuum polarization included in the self-consistent process. Retardation is also applied to Lorentz's and Coulomb's gauges.

The template is now formatted in order to perform the calculation for the desired level. The element's atomic number and the electron configuration are selected with the former having the same format as in Annex I. The double of the value of the total angular momentum is then indicated (as not to work with non-integer values) and so is the Lagrange multiplier/eigenvalue.

There are many other parameters to chose in order to have the `.f05` ready for the computation. These parameters, however, are not always the same, since occasionally different methods will have to be employed in order to reach convergence. Before these methods are discussed, it is necessary to provide an explanation as to how to evaluate the numerical convergence of the calculation:

2.3.3 Level calculation with *MCDFGME* - Alternative

For a given set of quantum numbers, a relativistic *MCDF* was performed using the *MCDFGME* script. The code executes an iterative self-consistent field calculation, accounting for both Coulomb and Breit's interactions, including the magnetic and retardation parts for the latter. For QED corrections, the formation of local potentials due to vacuum polarization was included in the self-consistent part of the calculation, while corrections due to self-energy were treated as perturbation. Furthermore, electron correlation was also accounted for by composing the antisymmetric wavefunction as a linear combination of state wavefunctions.

For executing the calculation, a previously tailored `.f05` input file is prepared. In it, a calculation with all the previously mentioned interactions is set up, with the option of changing the initial trial wavefunctions and the parameters of the self-consistent calculation

cycles. Throughout the calculation these wavefunctions will go through a variational process, changing until the optimal solution is reached, as can be observed in Figure 2.2.

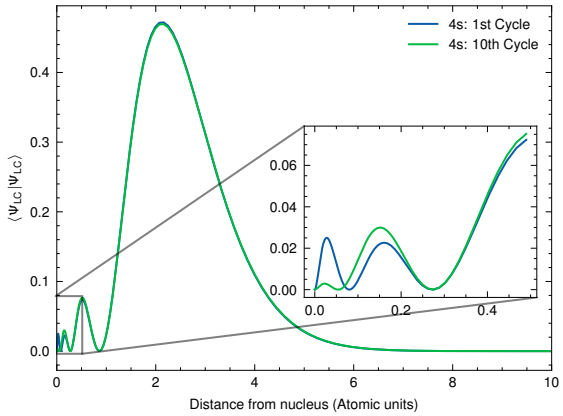

Figure 2.2: Wavefunction at the beginning and end of the self-consistent iterative process.

2.3.3.1 Evaluating the convergence

After launching the `mcdfgme2019.exe` executable, the computation will start, generating an output file with the `.f06` extension, where the output will be written while the program is actively running.

One of the convergence benchmarks can already be evaluated while the calculation is being processed. Actively monitoring the output file with, as an example, the `UNIX` command `tail`, one can observe some output from the self-consistent cycles. Should the numerical method not be reaching proper convergence, some warnings concerning sudden shifts in the wavefunction derivative may be displayed.

The calculation can also be aborted due to a numerical error. In this case, if the error occurred while running calculations for a certain orbital(s), this/these will be displayed on the error output.

The three other parameters used when evaluating if the convergence was successful can be checked only after the calculation is over:

- Each cycle, a component of the level's energy is calculated through two different methods. These two values should be consulted for the last cycle and the absolute energy difference should be below a certain stipulated benchmark value (1 eV).

- The wavefunction overlaps between each orbital sharing the same l_j value are displayed, since these cases are the most probable of having a convergence error leading them not to be orthogonal. The convergence is considered acceptable if every value is lower than 10^{-6}.

- For every orbital, the effective charge is calculated and displayed. This parameter is related to the shielding effect the charge of the electrons in other orbitals exert

on the nuclear charge. If the calculation converged correctly, these values should never be equal to the extreme possible values: 1 or N, where N is the total number of electrons. For each orbital, this value should be close to an expected value .

Meter aqui ref de como calcular

2.3.3.2 Level convergence methods

First attempt at numerical convergence For the first calculation, by default, a simpler template file (Annex II) is used and a calculation of five self-consistent cycles is performed. All trial orbital wavefunctions are initialized by wavefunctions calculated using the Thomas Fermi potential [37].

Second attempt at numerical convergence Should the first attempt have failed to reach convergence, a similar calculation is performed, keeping the previous parameters, but increasing the number of self-consistent cycles to 10, enforcing for each, an increasingly more precise accuracy and higher number of iterations. The template can be found in Annex III.

Third attempt at numerical convergence Should the previous two attempts have been made, and no convergence was reached, a new calculation needs to be made. In addition to the change cycle parameters, the parameters for some orbitals are to be altered. This can be done by altering the initial wavefunction to hydrogenics, or to a previously computed one. The method for solving the Dirac equation can also be changed for each chosen orbital. This final attempt can be quite time-consuming due to the many possibilities and combinations of methods to be employed for each orbital.

Since for every different studied system there are thousands of levels associated to it, a parallelized automation script was used. In total two scripts were used: a first one, previously written in `bash` by one of the advisors, Jorge Machado, which used the `parallel UNIX` command for parallelization, was used for the first calculations performed; and for most of the calculations, a new script, developed in the scope of this thesis, written in `Python` and employing an `MPI` approach for the purpose of parallelization. This last one will be discussed further in the thesis.

In the total number of calculated 1-hole and 2-holes levels is displayed in Table 2.3.

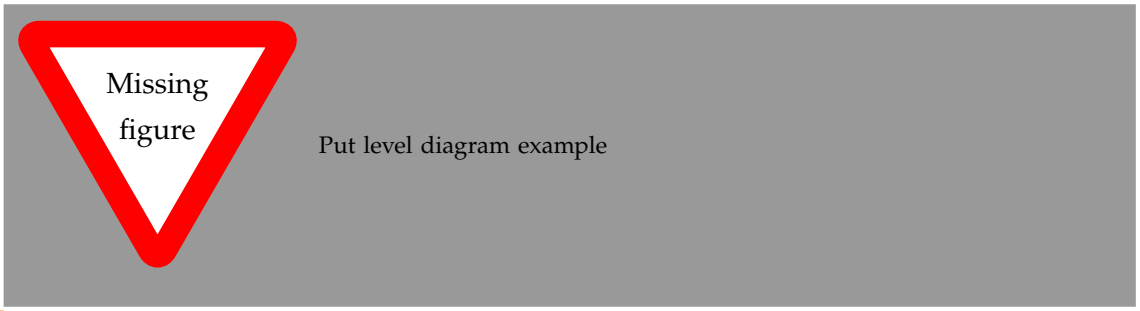

Maybe put a plot of the calculated wavefunctions

Table 2.3: Total number of levels calculated. For all but the first row, the orbital represented is the one where an electron was excited to.

Atomic	Number of levels			Number of hand-converged levels		
System	1-hole	2-holes	Total	1-hole	2-holes	Total
Cu^{1+}	19	183	202	0	1	1
4s						
4p	83	1001	1084	17	118	135
4d						
4f						
5s						
5p						
5d						
5f						
5g						
6s						
6p						
6d						
6f						
6g						
6h						
7p						
8p						
9p						
Total						

2.4 Transition computations

2.4.1 Diagram transitions

2.4.2 Auger transitions

2.4.3 Satellite transitions

2.4.3.1 Rate Matrices as a calculation evaluating comparison tool

Chapter 3

A new High-Performance Computing code for the parallelization of atomic structure calculations

3.1 A brief introduction on *MPI*

3.2 Program advantages

3.3 Program limitations

Blocking communication
CPU overheat
No buffering for now

Chapter 4

Fundamental atomic parameters calculation

asdas

Chapter 5

Spectra simulation

asdas

Chapter 6

Spectra analysis

6.1 Photoexcitation cross-section estimation

6.2 Photoionization cross-section computation

Chapter 7

Comparison with experimental data

Chapter 8

Next Steps

Chapter 9

Final remarks and Conclusion

Usar o Definitions aqui

9.1 Quantum states and properties

9.2 State transitions

9.2.1 Transition rates and widths

9.2.2 Branching Ratios and Fluorescence Yields

9.3 Spectra simulation

Chapter 10

Spectra Analysis

Chapter 11

Development of a HPC script for the parallelization of ASC

11.1 blablabla

11.2 Speedup

Compare with Amdahl's law or Gustafson's law.

Comparação com o do Jorge

Bibliography

[1] T. D. Thomas. "Transition from Adiabatic to Sudden Excitation of Core Electrons". In: *Phys. Rev. Lett.* 52 (6 1984), pp. 417–420. DOI: 10.1103/PhysRevLett.52.417. URL: https://link.aps.org/doi/10.1103/PhysRevLett.52.417 (cit. on p. 4).

[2] M. F. Vitha, R. Klockenkämper, and A. V. Bohlen. *Chemical Analysis: A Series of Monographs on Analytical Chemistry and Its Applications Total-Relection X-ray Fluorescence Analysis and Related Methods*. 2nd Edition. Vol. 181. 2015, pp. 20–21 (cit. on pp. 5, 37).

[3] *Hartree Fock method: A simple explanation*. URL: https://insilicosci.com/hartree-fock-method-a-simple-explanation/ (cit. on p. 7).

[4] J. P. Santos. *FÍSICA ATÓMICA Apontamentos para a UC FA 2020/21* (cit. on p. 7).

[5] R. Gabriel and T. Rosa. *The Hartree-Fock Method* (cit. on p. 7).

[6] S. M. Blinder. *Introduction to the hartree-fock method*. 2018-01. DOI: 10.1016/B978-0-12-813651-5.00001-2 (cit. on p. 7).

[7] B. Thaller. *The Dirac Equation*. Springer Berlin Heidelberg, 1992. DOI: 10.1007/978-3-662-02753-0 (cit. on p. 8).

[8] H. F. Beyer and V. P. Shevelko. *Introduction to the physics of highly charged ions*. IOP Pub, 2016, pp. 1–361. ISBN: 9781420034097. DOI: 10.1016/s0168-9002(03)00733-2 (cit. on p. 8).

[9] J. J. Sakurai and J. Napolitano. *Modern Quantum Mechanics*. Cambridge University Press, 2020-09. DOI: 10.1017/9781108587280 (cit. on p. 8).

[10] H. A. Bethe and E. E. Salpeter. *Quantum Mechanics of One- and Two-Electron Atoms*. Springer US, 1977. DOI: 10.1007/978-1-4613-4104-8 (cit. on pp. 8, 11).

[11] M. Strickland. *Relativistic Quantum Field Theory, Volume 1*. 2053-2571. Morgan & Claypool Publishers, 2019. ISBN: 978-1-64327-702-8. DOI: 10.1088/2053-2571/ab30cc. URL: https://dx.doi.org/10.1088/2053-2571/ab30cc (cit. on p. 9).

[12] P. A. M. Dirac. "The quantum theory of the electron". In: *Proceedings of the Royal Society of London. Series A, Containing Papers of a Mathematical and Physical Character* 117 (778 1928-02), pp. 610–624. ISSN: 0950-1207. DOI: 10.1098/rspa.1928.0023 (cit. on p. 9).

[13] D. Bank. *Atomic physics at GSI / FAIR:current and future research*. 2023-08 (cit. on p. 12).

[14] T. V. Nguyen et al. "Theory of copper K_α and K_β diagram lines, satellite spectra, and ab initio determination of single and double shake probabilities". In: *Physics Letters, Section A: General, Atomic and Solid State Physics* 426 (2022-02), p. 127900. ISSN: 03759601. DOI: 10.1016/j.physleta.2021.127900. URL: https://linkinghub.elsevier.com/retrieve/pii/S0375960121007659 (cit. on pp. 12, 13).

[15] H. A. Melia et al. "The characteristic radiation of copper K_β including radiative Auger processes". In: *Journal of Physics B: Atomic, Molecular and Optical Physics* 53 (19 2020-10), p. 195002. ISSN: 13616455. DOI: 10.1088/1361-6455/aba3a6. URL: https://iopscience.iop.org/article/10.1088/1361-6455/aba3a6 (cit. on p. 12).

[16] H. A. Melia et al. "The characteristic radiation of copper K_α 1,2,3,4". In: *Acta Crystallographica Section A: Foundations and Advances* 75 (3 2019-05), pp. 527–540. ISSN: 20532733. DOI: 10.1107/S205327331900130X. URL: http://www.ncbi.nlm.nih.gov/pubmed/31041908 (cit. on p. 12).

[17] H. Sorum. "The K_α1,2 X-ray spectra of the 3d transition metals Cr, Fe, Co, Ni and Cu". In: *Journal of Physics F: Metal Physics* 17 (2 1987-02), pp. 417–425. ISSN: 03054608. DOI: 10.1088/0305-4608/17/2/011 (cit. on p. 12).

[18] J. Bremer, T. Johnsen, and H. Sørum. "The Cu K_α1,2 spectrum as measured with a curved-crystal spectrometer". In: *X-Ray Spectrometry* 11 (3 1982), pp. 149–152. ISSN: 10974539. DOI: 10.1002/xrs.1300110312 (cit. on p. 12).

[19] M. Deutsch et al. "K and K x-ray emission spectra of copper". In: *Physical Review A* 51 (1 1995-01), pp. 283–296. ISSN: 10502947. DOI: 10.1103/PhysRevA.51.283 (cit. on p. 12).

[20] Y. Ito et al. "K_α1,2 x-ray linewidths, asymmetry indices, and [KM] shake probabilities in elements Ca to Ge and comparison with theory for Ca, Ti, and Ge". In: *Physical Review A* 94 (4 2016-10), p. 042506. ISSN: 24699934. DOI: 10.1103/PhysRevA.94.042506 (cit. on p. 13).

[21] H. Berger. "Study of the K_α emission spectrum of copper". In: *X-Ray Spectrometry* 15 (4 1986-10), pp. 241–243. ISSN: 0049-8246. DOI: 10.1002/xrs.1300150405. URL: https://onlinelibrary.wiley.com/doi/10.1002/xrs.1300150405 (cit. on p. 13).

[22] S. Galambosi et al. "Near-threshold multielectronic effects in the Cu $K_{\alpha_{1,2}}$ x-ray spectrum". In: *Physical Review A - Atomic, Molecular, and Optical Physics* 67 (2 2003-02), p. 5. ISSN: 10941622. DOI: 10.1103/PhysRevA.67.022510. URL: https://link.aps.org/doi/10.1103/PhysRevA.67.022510 (cit. on p. 13).

[23] C. T. Chantler, A. C. Hayward, and I. P. Grant. "Theoretical Determination of Characteristic X-Ray Lines and the Copper K_α Spectrum". In: *Physical Review Letters* 103 (12 2009-09), p. 123002. ISSN: 00319007. DOI: 10.1103/PhysRevLett.103.123002. URL: https://journals.aps.org/prl/abstract/10.1103/PhysRevLett.103.123002 (cit. on p. 13).

[24] F. Gel'mukhanov and H. Ågren. *Resonant X-ray Raman scattering*. Vol. 312. Elsevier, 1999, pp. 87–330. DOI: 10.1016/S0370-1573(99)00003-4 (cit. on p. 13).

[25] P. Carra, M. Fabrizio, and B. T. Thole. "High resolution x-ray resonant Raman scattering". In: *Physical Review Letters* 74 (18 1995-05), pp. 3700–3703. ISSN: 00319007. DOI: 10.1103/PhysRevLett.74.3700 (cit. on p. 13).

[26] P. Eisenberger, P. M. Platzman, and H. Winick. "X-ray resonant Raman scattering: Observation of characteristic radiation narrower than the lifetime width". In: *Physical Review Letters* 36 (11 1976-03), pp. 623–626. ISSN: 00319007. DOI: 10.1103/PhysRevLett.36.623 (cit. on p. 13).

[27] P. Indelicato, J. Bieroń, and P. Jönsson. "Are MCDF calculations 101% correct in the super-heavy elements range?" In: *Theoretical Chemistry Accounts* 129 (3-5 2011-06), pp. 495–505. ISSN: 1432881X. DOI: 10.1007/s00214-010-0887-3 (cit. on p. 13).

[28] P. Indelicato, O. Gorveix, and J. P. Desclaux. "Multiconfigurational Dirac-Fock studies of two-electron ions. II. Radiative corrections and comparison with experiment". In: *Journal of Physics B: Atomic and Molecular Physics* 20 (4 1987-02), p. 651. ISSN: 0022-3700. DOI: 10.1088/0022-3700/20/4/007 (cit. on p. 13).

[29] O. Gorceix, P. Indelicato, and J. P. Desclaux. "Multiconfiguration Dirac-Fock studies of two-electron ions. I. Electron-electron interaction". In: *Journal of Physics B: Atomic and Molecular Physics* 20 (4 1987-02), pp. 639–649. ISSN: 00223700. DOI: 10.1088/0022-3700/20/4/006 (cit. on p. 13).

[30] M. Guerra et al. "Fundamental Parameters Related to Selenium Kα and Kβ Emission X-ray Spectra". In: *Atoms* 9 (1 2021-01), p. 8. ISSN: 2218-2004. DOI: 10.3390/atoms9010008. URL: https://www.mdpi.com/2218-2004/9/1/8 (cit. on p. 13).

[31] N. Paul et al. "Testing Quantum Electrodynamics with Exotic Atoms". In: *Physical Review Letters* 126 (17 2021-04), p. 173001. ISSN: 10797114. DOI: 10.1103/PhysRevLett.126.173001 (cit. on p. 13).

[32] M. F. Gu. *The flexible atomic code*. 2008-05. DOI: 10.1139/P07-197 (cit. on p. 13).

[33] P. Jönsson et al. "New version: Grasp2K relativistic atomic structure package". In: *Computer Physics Communications* 184 (9 2013-09), pp. 2197–2203. ISSN: 00104655. DOI: 10.1016/j.cpc.2013.02.016 (cit. on p. 13).

[34] *ASCL.net - AUTOSTRUCTURE: General program for calculation of atomic and ionic properties*. URL: https://ascl.net/1612.014 (cit. on p. 13).

[35] J. P. Desclaux and P. Indelicato. *Input data for relativistic atomic program MCDF V 2019.1*. 2019 (cit. on p. 14).

[36] *Metrology of simple systems and fundamental tests*. URL: https://www.lkb.upmc.fr/metrologysimplesystems/mdfgme-a-general-purpose-multiconfiguration-dirac-foc-program/ (cit. on p. 14).

[37] L. H. Thomas. "The calculation of atomic fields". In: *Mathematical Proceedings of the Cambridge Philosophical Society* 23.5 (1927), 542–548. DOI: 10.1017/S0305004100011683 (cit. on p. 20).

[38] W. E. Lamb and R. C. Retherford. "Fine structure of the hydrogen atom by a microwave method". In: *Physical Review* 72 (3 1947-08), pp. 241–243. ISSN: 0031899X. DOI: 10.1103/PhysRev.72.241 (cit. on p. 38).

Appendix A

The Breit Hamiltonian Operators

Note: This operators are valid for the electrons in an atom.
The free particle energy:

$$H_0 = \sum_i^N \frac{p^2}{2m_e} \tag{A.1}$$

The electron-nucleus Coulomb attraction:

$$H_1 = \sum_i^N -\frac{e^2 Z}{r_i} \tag{A.2}$$

The electron-electron Coulomb repulsion:

$$H_2 = \sum_{i<j} \frac{e^2}{r_{ij}} \tag{A.3}$$

Incorporates the relativistic apparent mass - velocity dependance:

$$H_3 = -\frac{1}{8{m_e}^3 c^2} \sum_i^N p_i^4 \tag{A.4}$$

Electric field retardation and magnetic dipole interaction:

$$H_4 = -\frac{e^2}{2{m_e}^2 c^2} \sum_{i<j} \left[\frac{\boldsymbol{p}_i \cdot \boldsymbol{p}_j}{r_{ij}} + \frac{\left(\boldsymbol{r_{ij}} \cdot \boldsymbol{p}_{ij}\right)\left(\boldsymbol{r}_{ij} \cdot \boldsymbol{p}_j\right)}{{r_{ij}}^3} \right] \tag{A.5}$$

Darwin's term, accounts for the electron's quantum fluctuation motion:

$$H_5 = \frac{\pi e \hbar^2}{2{m_e}^2 c^2} \sum_{i<j} \frac{Z}{2} \left[\delta(\boldsymbol{r}_i) + \delta\left(\boldsymbol{r}_j\right) \right] + \delta\left(\boldsymbol{r}_{ij}\right) \tag{A.6}$$

And the last two operators, for the consideration of spin orbit interactions:

$$H_6 = \frac{e^2\hbar^2}{2{m_e}^2c^2}\sum_{i<j}\left(Z\frac{\boldsymbol{r}_i \times \boldsymbol{p}_i}{{r_i}^3} - \frac{\boldsymbol{r}_{ij} \times \boldsymbol{p}_i}{{r_{ij}}^3} + 2\frac{\boldsymbol{r}_{ij} \times \boldsymbol{p}_j}{{r_{ij}}^3}\right)\boldsymbol{s}_i + \left(Z\frac{\boldsymbol{r}_j \times \boldsymbol{p}_j}{{r_j}^3} - \frac{\boldsymbol{r}_{ji} \times \boldsymbol{p}_j}{{r_{ij}}^3} + 2\frac{\boldsymbol{r}_{ji} \times \boldsymbol{p}_i}{{r_{ij}}^3}\right)\boldsymbol{s}_j \tag{A.7}$$

$$H_7 = \frac{e^2\hbar^2}{{m_e}^2c^2}\sum_{i<j}\left(-\frac{8\pi}{3}\boldsymbol{s}_i \cdot \boldsymbol{s}_j\,\delta\left(\boldsymbol{r}_{ij}\right) + \frac{1}{{\boldsymbol{r}_{ij}}^3}\left[\boldsymbol{s}_i \cdot \boldsymbol{s}_j - \frac{3\left(\boldsymbol{s}_i \cdot \boldsymbol{r}_{ij}\right)\left(\boldsymbol{s}_j \cdot \boldsymbol{r}_{ij}\right)}{{\boldsymbol{r}_{ij}}^2}\right]\right) \tag{A.8}$$

Appendix B

Transition Diagram

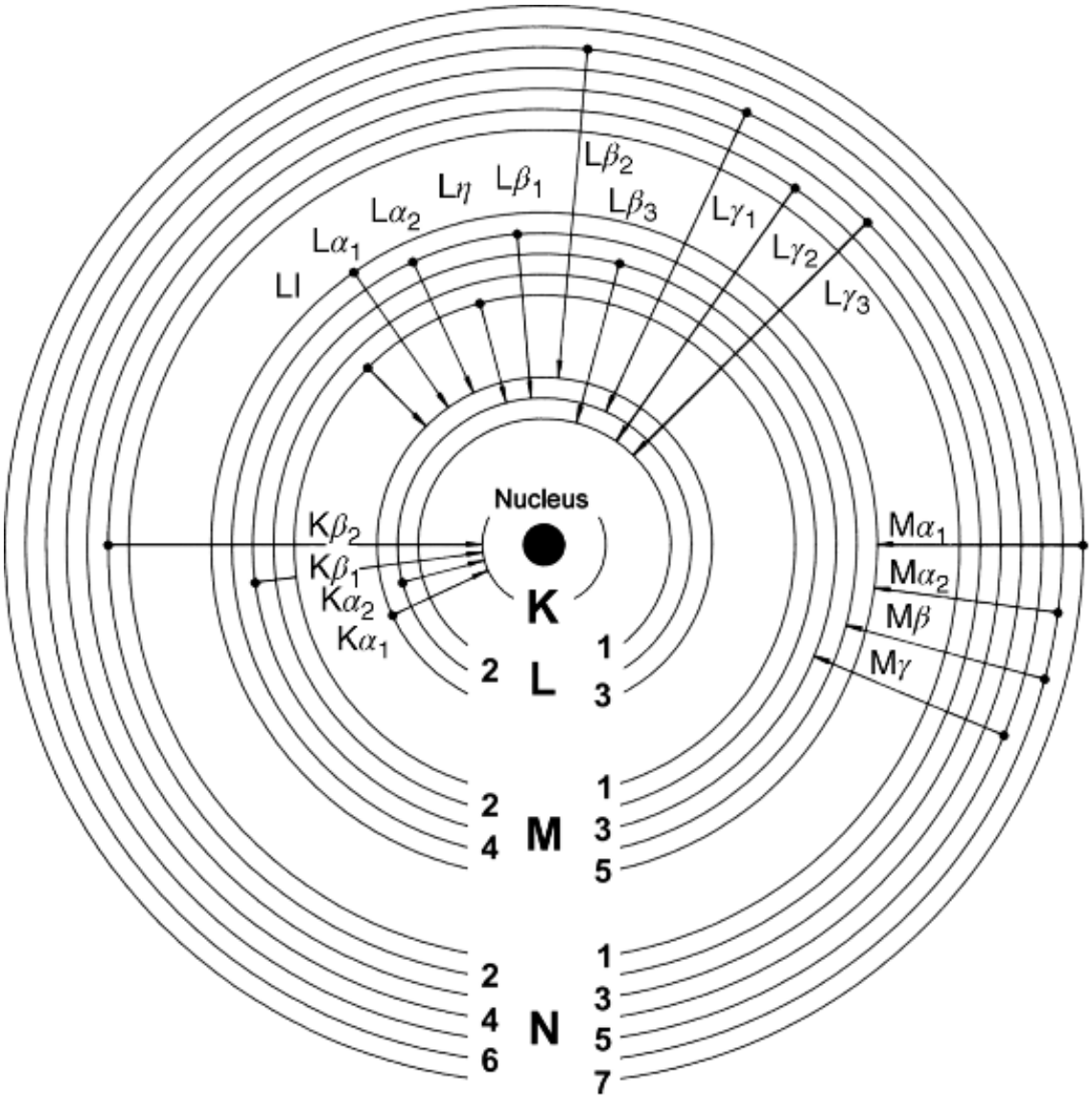

Figure B.1: Transition notation scheme. Adapted from [2]

Appendix C

QED considerations

It should be apparent by now that studying Atomic systems call not only for relativistic effects and corrections, but also for QED ones.

One of the most famous cases where QED came to light was the discovery of the Lamb Shift [38], when it was discovered Hydrogen's $2s_{1/2}$ and $2p_{1/2}$ levels were in fact, not degenerate (did not have the same energy), contrary to what was expected from solving Dirac's equation. This difference in energy came to be known as the Lamb Shift, only explained by QED effects.

C.1 Self-Energy

The self-energy represents a particle's emission and reabsorption of virtual photon, present in the particle's own generated field. This interaction has the most impact in the Lamb Shift effect and when performing energy corrections. One of its Feynman Diagrams can be seen in Figure C.1a.

C.2 Vacuum Polarization

As previously stated, electromagnetic fields, such as the Coulomb field generated by the nucleus, are mediated by virtual photons. These photons can lead to the creation of electron-positron pairs which create screening effects. Pair annihilation will follow, leading to the production of another virtual photon (Figure C.1b).

(a) Self Energy (b) Vacuum Polarization

Figure C.1: QED Feynman Diagrams

4p excited Copper configurations

I.1 1-hole configurations

```
    (1s)1 (2s)2 (2p)6 (3s)2 (3p)6 (4s)1 (3d)10 (4p)1 ,1s
    (1s)2 (2s)1 (2p)6 (3s)2 (3p)6 (4s)1 (3d)10 (4p)1 ,2s
    (1s)2 (2s)2 (2p)5 (3s)2 (3p)6 (4s)1 (3d)10 (4p)1 ,2p
    (1s)2 (2s)2 (2p)6 (3s)1 (3p)6 (4s)1 (3d)10 (4p)1 ,3s
    (1s)2 (2s)2 (2p)6 (3s)2 (3p)5 (4s)1 (3d)10 (4p)1 ,3p
    (1s)2 (2s)2 (2p)6 (3s)2 (3p)6 (4s)1 (3d)9 (4p)1  ,3d
    (1s)2 (2s)2 (2p)6 (3s)2 (3p)6 (3d)10 (4p)1       ,4s
    (1s)2 (2s)2 (2p)6 (3s)2 (3p)6 (4s)1 (3d)10       ,4p
```

I.2 2-holes configurations

```
    (2s)2 (2p)6 (3s)2 (3p)6 (3d)10 (4s)1 (4p)1       ,1s_1s
    (1s)1 (2s)1 (2p)6 (3s)2 (3p)6 (3d)10 (4s)1 (4p)1 ,1s_2s
    (1s)1 (2s)2 (2p)5 (3s)2 (3p)6 (3d)10 (4s)1 (4p)1 ,1s_2p
    (1s)1 (2s)2 (2p)6 (3s)1 (3p)6 (3d)10 (4s)1 (4p)1 ,1s_3s
    (1s)1 (2s)2 (2p)6 (3s)2 (3p)5 (3d)10 (4s)1 (4p)1 ,1s_3p
    (1s)1 (2s)2 (2p)6 (3s)2 (3p)6 (3d)9 (4s)1 (4p)1  ,1s_3d
    (1s)1 (2s)2 (2p)6 (3s)2 (3p)6 (3d)10 (4p)1       ,1s_4s
    (1s)1 (2s)2 (2p)6 (3s)2 (3p)6 (3d)10 (4s)1       ,1s_4p
    (1s)2 (2p)6 (3s)2 (3p)6 (3d)10 (4s)1 (4p)1       ,2s_2s
    (1s)2 (2s)1 (2p)5 (3s)2 (3p)6 (3d)10 (4s)1 (4p)1 ,2s_2p
    (1s)2 (2s)1 (2p)6 (3s)1 (3p)6 (3d)10 (4s)1 (4p)1 ,2s_3s
    (1s)2 (2s)1 (2p)6 (3s)2 (3p)5 (3d)10 (4s)1 (4p)1 ,2s_3p
    (1s)2 (2s)1 (2p)6 (3s)2 (3p)6 (3d)9 (4s)1 (4p)1  ,2s_3d
    (1s)2 (2s)1 (2p)6 (3s)2 (3p)6 (3d)10 (4p)1       ,2s_4s
    (1s)2 (2s)1 (2p)6 (3s)2 (3p)6 (3d)10 (4s)1       ,2s_4p
    (1s)2 (2s)2 (2p)4 (3s)2 (3p)6 (3d)10 (4s)1 (4p)1 ,2p_2p
    (1s)2 (2s)2 (2p)5 (3s)1 (3p)6 (3d)10 (4s)1 (4p)1 ,2p_3s
    (1s)2 (2s)2 (2p)5 (3s)2 (3p)5 (3d)10 (4s)1 (4p)1 ,2p_3p
    (1s)2 (2s)2 (2p)5 (3s)2 (3p)6 (3d)9 (4s)1 (4p)1  ,2p_3d
    (1s)2 (2s)2 (2p)5 (3s)2 (3p)6 (3d)10 (4p)1       ,2p_4s
    (1s)2 (2s)2 (2p)5 (3s)2 (3p)6 (3d)10 (4s)1       ,2p_4p
```

```
22     (1s)2 (2s)2 (2p)6 (3p)6 (3d)10 (4s)1 (4p)1       ,3s_3s
23     (1s)2 (2s)2 (2p)6 (3s)1 (3p)5 (3d)10 (4s)1 (4p)1 ,3s_3p
```

ANNEX II

First cycle template

```
program_year=2019 program_version=1
*   1 mcdfgmelabel
    scfmdf max  :
    mod_lightspeed=n
    nz=mcdfgmeatomicnumber
    mdf  opt_ener=todo  modfilname_ener=n modfilname_wf=n do_scf=y
    Breit=full  mag_scf=y  ret_scf=y
    qedstpg_n4=n
    vacpol_scf=y
    energy
#    use_mcdfener=y
#    opt_relax=y
    ret_Lorentz=y
    opt_qedel=y :
# ":" above is for ilams taken to be the default value
    mod_mesh=n
#    hx=0.012 r(1)=0.001 amesh=0.01 :
    exotic=n
    use_nms=y
    mod_nuc=n
    project=n
#    cgt_order_vint=y order=6
    cgt_order_vint=n
    def_config=given
    nbel=mcdfgmeelectronnb jjt=mcdfgmejj  :
c  1 mcdfgmeconfiguration:
end
# initial state parameters
    neigv=mcdfgmeneigv   icmul=0   iprfgr=0
    norbsc=00  ndep=0   nlec=0   nec=1  :
    nstep=0
    lregul=n  modtest=n
    modsolv_orb=n
    mod_odlm=n
# data for uwfrdf
```

```
36          :
37      **
```

ANNEX III

Input File .f05 Example

```
program_year=2019 program_version=1
*   1 mcdfgmelabel
    scfmdf max  :
    mod_lightspeed=n
    nz=mcdfgmeatomicnumber
    mdf  opt_ener=todo  modfilname_ener=n modfilname_wf=n do_scf=y
    Breit=full  mag_scf=y  ret_scf=y
    qedstpg_n4=n
    vacpol_scf=y
    energy
#    use_mcdfener=y
#    opt_relax=y
    ret_Lorentz=y
    opt_qedel=y :
# ":" above is for ilams taken to be the default value
    mod_mesh=n
#    hx=0.012 r(1)=0.001 amesh=0.01 :
    exotic=n
    use_nms=y
    mod_nuc=n
    project=n
#    cgt_order_vint=y order=6
    cgt_order_vint=n
    def_config=given
    nbel=mcdfgmeelectronnb jjt=mcdfgmejj  :
c  1 mcdfgmeconfiguration:
end
# initial state parameters
    neigv=mcdfgmeneigv   icmul=0   iprfgr=0
    norbsc=00  ndep=0   nlec=0   nec=1  :
    nstep=10
    n y y  50  z=mcdfgmeatomicnumber  1.D-2  0.2  1.  1.
    n y y  50  z=mcdfgmeatomicnumber  3.D-3  0.2  1.  1.
    n y y  50  z=mcdfgmeatomicnumber  1.D-3  0.3  1.  1.
    n y y  50  z=mcdfgmeatomicnumber  3.D-4  0.3  1.  1.
```

```
      n y y  50  z=mcdfgmeatomicnumber  1.D-4  0.5  1.  1.
      n y y  50  z=mcdfgmeatomicnumber  3.D-5  0.5  1.  1.
      n y y  50  z=mcdfgmeatomicnumber  1.D-5  0.5  1.  1.
      n y y  100  z=mcdfgmeatomicnumber  4.D-6  1.  1.  1.
      n y y  100  z=mcdfgmeatomicnumber  2.D-6  1.  1.  1.
      n y y  200  z=mcdfgmeatomicnumber  1.D-6  1.  1.  1.
      lregul=n  modtest=n
      modsolv_orb=n
      mod_odlm=n
  # data for uwfrdf
      :
  **
```